Deconvolution-based super-resolution for post-adaptive-optics data

M. Carbillet[1], A. La Camera[2], O. Chesneau[3], F. Millour[3], J. H. V. Girard[4], M. Prato[5]

[1]: UMR 7293 Lagrange (Université de Nice Sophia-Antipolis/CNRS/Observatoire de la Côte d'Azur), Parc Valrose, 06100 Nice, France → marcel.carbillet@unice.fr.
[2]: Dipartimento di Informatica, Bioingegneria, Robotica e Ingegneria dei Sistemi (Università di Genova), Via Dodecaneso 35, 16145 Genova, Italia → andrea.lacamera@unige.it.
[3]: UMR 7293 Lagrange (Université de Nice Sophia-Antipolis/CNRS/Observatoire de la Côte d'Azur), Boulevard de l'Observatoire, BP 4229, 06300 Nice, France.
[4]: European Southern Observatory, Casilla 19001, Vitacura, Santiago, Chile.
[5]: Dipartimento di Scienze Fisiche, Informatiche e Matematiche (Università di Modena e Reggio Emilia), Via Campi 213/b, 41125 Modena, Italia.

Abstract This poster presents preliminary results on NACO/VLT images of close binary stars obtained by means of a Richardson-Lucy-based algorithm of super-resolution, where down to less than a half-resolution element is attained, and with confirmation from VLTI observations in one of the cases treated. A new gradient method, the scaled gradient projection (SGP), permitting the acceleration of the used method, is also tested with the same scope.

Richardson-Lucy deconvolution method

We define $\mathbf{f}$ as the scientific target, $\mathbf{g}$ the acquired image to be deconvolved, $\mathbf{b}$ the sky background, and A the imaging matrix given by $A\mathbf{f} = \mathbf{K} * \mathbf{f}$, where $*$ is the convolution operator and K is the point-spread function (PSF), normalized to a unit volume. In the case of Poisson noise, the general approach to the deconvolution methods follows the minimization of the Kullback-Leibler (KL) divergence given by:

$$J_0(\mathbf{f};\mathbf{g}) = \sum_{\mathbf{m}\in S}\left\{\mathbf{g}(\mathbf{m})\ln\frac{\mathbf{g}(\mathbf{m})}{(A\mathbf{f})(\mathbf{m})+\mathbf{b}(\mathbf{m})} + (A\mathbf{f})(\mathbf{m}) + \mathbf{b}(\mathbf{m}) - \mathbf{g}(\mathbf{m})\right\} .$$

From well-known properties of this functional, it follows that J_0 is *non-negative*, *convex*, and *coercive*. So that absolute minimizers of this function exist: the so-called *maximum likelihood* (ML) solutions of the image reconstruction problem. The Richardson-Lucy (RL) method [1, 2] follows from the computation of the gradient of J_0 and the application of the Karush-Kuhn-Tucker conditions. It is described in Algorithm 1.

Algorithm 1 RL method

Choose the starting point $\mathbf{f}^{(0)} \geq 0$

FOR $k = 0, 1, 2, \ldots$ COMPUTE:

$$\mathbf{f}^{(k+1)} = \mathbf{f}^{(k)} A^T \frac{\mathbf{g}}{A\mathbf{f}^{(k)} + \mathbf{b}}$$

END

Richardson-Lucy-based super-resolution

The global method used in this poster is based on the well-known property of RL which allows (computing) super-resolution [3, 4, 5]. It consists in the following two steps, as described in [6].

- STEP 1 - Compute a large number of RL iterations, assuming a constant array as initial guess of the algorithm. We denote the result of this step by $\mathbf{f_1}$.
- STEP 2 - Define the (compact) support $\mathcal{S}$ of the object as the pixels where the flux of $\mathbf{f_1}$ is greater than a selected threshold, or alternatively an area of angular dimension of the order of the resolution element of the data (more explicitly λ/D, where λ is the observing wavelength and D the diameter of the telescope). Next, initialize the algorithm using the mask with pixels set to one inside and to zero outside the domain $\mathcal{S}$. Then, compute again a large number of RL iterations, obtaining the final reconstructed image $\mathbf{f_2}$.

The super-resolution method described above and used in the following is implemented within the last distributed versions of the `Software Package AIRY` [7, 8], developed within the CAOS problem-solving environment [9, 10].

Scaled gradient projection acceleration

The RL algorithm can be seen as a particular case of a scaled gradient method. Indeed, since

$$\mathbf{f}^{(k+1)} = \mathbf{f}^{(k)} - \mathbf{f}^{(k)}\left(\mathbf{1} - A^T\frac{\mathbf{g}}{A\mathbf{f}^{(k)}+\mathbf{b}}\right) = \mathbf{f}^{(k)} - \mathbf{f}^{(k)}\nabla J_0(\mathbf{f}^{(k)};\mathbf{g}) ,$$

it follows that the RL iteration can be obtained from the general scaled gradient algorithm:

$$\mathbf{f}^{(k+1)} = \mathbf{f}^{(k)} - \lambda_k(P_+(\mathbf{f}^{(k)} - \alpha_k D_k \nabla J_0(\mathbf{f}^{(k)};\mathbf{g})) - \mathbf{f}^{(k)}) ,$$

by choosing the constant steplengths $\lambda_k = \alpha_k = 1$, the scaling matrix $D_k = \mathrm{diag}(\mathbf{f}^{(k)})$, and by remarking that for RL the projection P_+ on the non-negative pixels can be avoided since it is automatically satisfied by the iteration.

The choice of constant steplengths makes RL not very efficient and several acceleration schemes have been proposed in the literature to improve its convergence rate. The scaled gradient projection (SGP) method [11] is an optimization method for the minimization of the KL divergence that uses the scaling of the gradient suggested by RL, but exploits an adaptive strategy for the steplength parameters. For this reason, SGP can be considered as a more efficient version of RL.

The SGP scheme is described in Algorithm 2. For a general version of the algorithm and, in particular, for the computation of the steplength parameter α_k, we refer to [11, 12].

Algorithm 2 SGP method

Choose the starting point $\mathbf{f}^{(0)} \geq 0$ and set the parameters $\beta, \theta \in (0,1)$, $0 < \alpha_{min} < \alpha_{max}$.

FOR $k = 0, 1, 2, \ldots$ DO THE FOLLOWING STEPS:

STEP 1. Choose the parameter $\alpha_k \in [\alpha_{min}, \alpha_{max}]$ and the scaling matrix D_k;

STEP 2. Projection:

$$\mathbf{y}^{(k)} = P_+(\mathbf{f}^{(k)} - \alpha_k D_k \nabla J_0(\mathbf{f}^{(k)};\mathbf{g}));$$

STEP 3. Descent direction: $\mathbf{d}^{(k)} = \mathbf{y}^{(k)} - \mathbf{f}^{(k)}$;

STEP 4. Set $\lambda_k = 1$;

STEP 5. Backtracking loop:

IF $J_0(\mathbf{f}^{(k)} + \lambda_k \mathbf{d}^{(k)};\mathbf{g}) \leq J_0(\mathbf{f}^{(k)};\mathbf{g}) + \beta\lambda_k \nabla J_0(\mathbf{f}^{(k)};\mathbf{g})^T \mathbf{d}^{(k)}$
THEN go to step 6;
ELSE set $\lambda_k = \theta\lambda_k$ and go to step 5.
ENDIF

STEP 6. Set $\mathbf{f}^{(k+1)} = \mathbf{f}^{(k)} + \lambda_k \mathbf{d}^{(k)}$.

END

The super-resolution acceleration can be obtained applying the same scheme described in the previous section, replacing RL with SGP. The SGP method will be implemented in the next distributed version of the `Software Package AIRY`. We apply in the following the two methods described to NACO/VLT data of very close binary stars, but in the case of SGP we push the algorithm to convergence, i.e. we compute the *objective function* $J_0(\mathbf{f}^{(k)};\mathbf{g})$ at each iteration and we stop the iteration when this function is (almost) constant — i.e., according to a given tolerance ϵ, when $|J_0(\mathbf{f}^{(k)};\mathbf{g}) - J_0(\mathbf{f}^{(k-1)};\mathbf{g})| < \epsilon \cdot J_0(\mathbf{f}^{(k)};\mathbf{g})$.

Preliminary results on NACO/VLT data

→ HD 87643

The data considered here are K-band data obtained with NACO/VLT and already analyzed by Millour et al. [13] together with VLTI observations of the same object: HD 87643. A first deconvolution of the NACO/VLT data has already also been presented in Le Bouquin et al.[14], but in both cases the (very close) binary star could not have been resolved. At the opposite, in [13], the observations of the same object using the interferometric instrument AMBER onboard the VLTI clearly shown the binarity of the source.

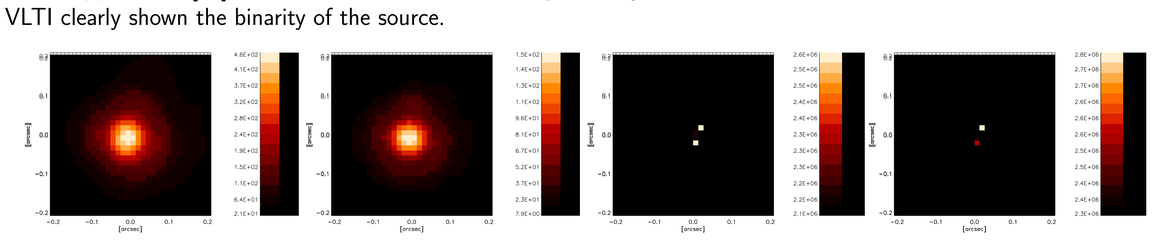

From left to right: first post-NACO image of HD 87643, corresponding PSF, super-resolution reconstruction, super-resolution SGP-accelerated reconstruction. The resolution element is here of $\lambda/D \simeq 56$ mas, i.e. a little bit more than 4.3 px with a pixel size of 13 mas. Found separation: $\rho \simeq 31$ mas $\simeq 2.4$ px $\simeq 0.55\,\lambda/D$.

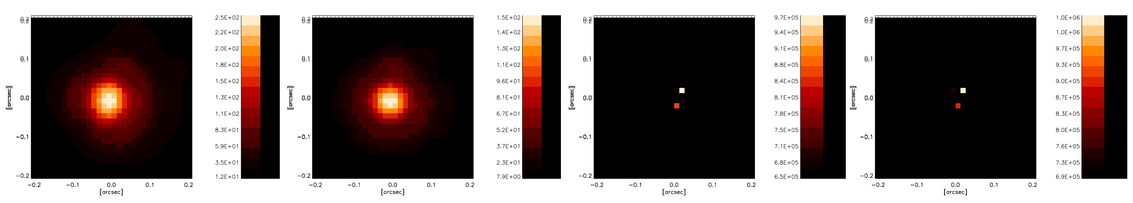

From left to right: second post-NACO image of HD 87643, corresponding PSF, super-resolution reconstruction, super-resolution SGP-accelerated reconstruction. The resolution element is here of $\lambda/D \simeq 56$ mas, i.e. a little bit more than 4.3 px with a pixel size of 13 mas. Found separation: $\rho \simeq 32$ mas $\simeq 2.45$ px $\simeq 0.57\,\lambda/D$.

The result from the two images considered here above are completely similar to the result obtained with AMBER/VLTI. Hence we can conclude that we have here fully validated our approach of (computing) super-resolution.

→ HIP 113010

The data considered here below are 4-μm data obtained again with NACO/VLT. The resolution element is $\lambda/D \simeq 103$ mas, i.e a little bit less than 3.8 px with a pixel size of $\simeq 27.2$ mas.

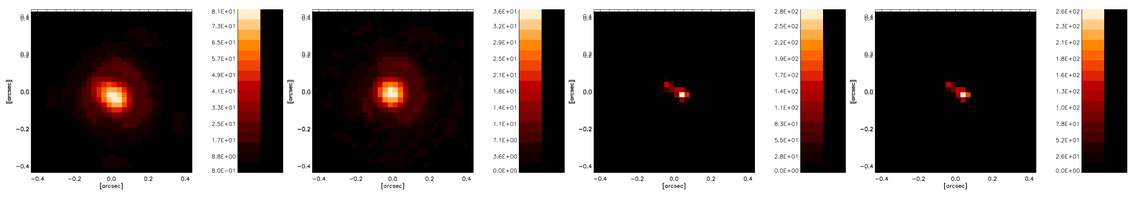

From left to right: post-NACO image of HIP 113010, corresponding PSF, super-resolution reconstruction, super-resolution SGP-accelerated reconstruction. Found separation: $\rho \simeq 84$ mas $\simeq 3.0$ px $\simeq 0.82\,\lambda/D$.

Although in this latter case the task is easier than previously because the binarity of the object can already could recognized in the pre-processed data (elongated shape clearly distinguishable from the PSF centro-symmetric shape), these results are also a matter for super-resolution.

→ Discussion

With the RL algorithm 5000 iterations were performed for the first step and 1000 iterations for the second step. With SGP, the number of iterations were between ~ 140 and ~ 590 for the first step and between~ 43 and ~ 150 for the second step. The results are very similar in both cases. Although the computational cost is heavier with SGP, we have at the end a resulting global speed-up between ~ 7.5 and ~ 24 when SGP is employed. In any case, and with such tiny regions of interest (in terms of number of pixels concerned by the object reconstruction process), computational times were in both cases quite small: between 14 s and 50 s for RL and between 0.6 s and 6.7 s for SGP, on an Intel Core 2 Duo at 2.4 GHz. It is nevertheless worthwhile to note that, with a dedicated camera, with much more pixels per resolution element in order to fully take advantage from the super-resolution method, this computational time gain would begin to be more interesting.
A last point concerns the photometric accuracy. No particular effort was made here, but our next-to-come step is to implement the third step of the procedure described in [6] and apply it to the data presented, permitting a priori a better reconstruction of the objects, and hopefully a quantitative comparison between the accuracies permitted with RL and SGP.

References

[1] W. H. Richardson 1972, J. Opt. Soc. Am. 62, 55.
[2] L. B. Lucy 1974, Astron. J. 79, 745.
[3] M. Bertero & C. De Mol 1996, E. Wolf Ed., Progress in Optics XXXVI, Chap. III, Elsevier, Amsterdam.
[4] M. Bertero & P. Boccacci 1998, in "Introduction to inverse problems in imaging", IoP Publishing, Bristol.
[5] M. Bertero & P. Boccacci 2002, in "Confocal and two-photon microscopy: foundations, applications, and advances", A. Diaspro Ed., Chap. 12.
[6] B. Anconelli et al. 2005, Astron. Astrophys. 431, 747.
[7] S. Correia et al. 2002, Astron. Astrophys. 387 (2), 733.
[8] A. La Camera et al. 2012, SPIE Proc. 8445, 84453E.
[9] M. Carbillet et al. 2004, SPIE Proc. 5490, 721.
[10] M. Carbillet et al. 2010, SPIE Proc. 7736, 773644.
[11] S. Bonettini et al. 2009, Inverse Prob., 25, 015002.
[12] M. Prato et al. 2012, Astron. Astrophys. 539, A133.
[13] F. Millour et al. 2009, Astron. Astrophys. 507, 317.
[14] J.-B. Le Bouquin et al. 2009, The Messenger 137, 25.

This study is being performed using the `Software Package AIRY`, see http://airyproject.eu, developed within the `CAOS problem-solving environment`, see http://lagrange.oca.eu/caos.